SUPPLEMENTAL MATERIAL

Methods

DNA

Human LITAF was cloned from human heart RNA (Agilent Technologies). The 3xHA-tagged open reading frame of LITAF was cloned into pENTR 1A Dual (Thermo Fisher). The LITAF open reading frame was then transferred to the vector pAd/CMV/V5-DEST (Thermo Fisher) using the Gateway cloning system (Thermo Fisher). 293A cells (Thermo Fisher) were transfected with *Pac*I-digested pAd/CMV/V5-DEST-LITAF-HA and adenoviral stocks were prepared according to the manufacturer. As control, we used the 'empty' vector pAd/CMV/V5-DEST-GFP that allows the expression of GFP.[1] To create adenovirus expressing shRNA against rabbit LITAF and NEDD4-1, the following strategy was used: The BLOCK-iT™ RNAi Designer (Thermo Fisher) was used to design suitable shRNA molecules driven by the U6 promoter of the Gateway entry vector pENTR™/U6 (Thermo Fisher). The expression cassettes consisting of U6 promoter, shRNA-encoding sequence and Pol III terminator was then transferred to the vector pAd/PL-DEST (Thermo Fisher) using the Gateway cloning system. 293A cells were transfected with *Pac*I-digested pAd/PL-DEST-LITAF-shRNA or pAd/PL-DEST-NEDD4-1-shRNA and adenoviral stocks were prepared according to the manufacturer. As control, we used a similar strategy to create the control vector pAd/PL-scrambled-control that allows the expression of scrambled RNA. The following DNA oligonucleotides (gene-specific sequences are underlined) were used for cloning: LITAF-shRNA: top: 5'-CACCGGTGGCCGTCAACAGTTACTACGAATAGTAACTGTTGACGGCCACC-3', bottom: 5'-AAAAGGTGGCCGTCAACAGTTACTATTCGTAGTAACTGTTGACGGCCACC-3'; NEDD4-1-shRNA: top: 5'-CACCGGAGTCAGTGGATAGTGAATACGAATATTCACTATCCACTGACTCC-3', bottom: 5'-AAAAGGAGTCAGTGGATAGTGAATATTCGTATTCACTATCCACTGACTCC-3'; scrambled-control: top: 5'-CACCGACCTAC-GCCTTAGACAGAGTATTCACGAGGAGAGACGGTTCTTTCA-3', bottom: 5'-AAAATGAAAGAACCGTCTCTCCTCGTGAATACTCTGTCTAAGGCGTAGGTC-3'.
3xHA- or 3xFlag-tagged LITAF open reading frames were cloned into pcDNA3 (Life Technologies). The following plasmids were purchased from Addgene: pRK5-HA-Ubiquitin-WT expressing HA-tagged ubiquitin, (Addgene ID 17608);[2] pcDNA6/V5-His-Cav1.2 expressing Cavα1c (Addgene ID 26572);[3] pcDNA3.1/Zeo-Cavb3 expressing Cavβ3 (Addgene ID 26574); pcDNA3.1/Zeo-CaVα2δ-1 expressing Cavα2δ-1 (Addgene ID 26575);[4] pCI-HA-NEDD4-DD expressing catalytically inactive HA-tagged NEDD4-1-C867A (Addgene ID 26999);[5] and pCI-HA-NEDD4 expressing HA-tagged NEDD4-1 (Addgene ID 27002).[5] The plasmid pEGFP was obtained from Clontech.

Transfections

Human embryonic kidney tsA201 cells (MilliporeSigma) were cultured in DMEM (Thermo Fisher), split at approximately 50% confluency and only used at low passage numbers. Transient transfections into tsA201 cells were performed using lipofectamine 2000 (Thermo Fisher) following the manufacturer's instructions.

Preparation of rabbit cardiomyocytes

All animal experiments and procedures were approved by the Rhode Island Hospital Institutional Animal Care and Use Committee (reference numbers: 0188-14 and 5013-17).

Adult septal cardiomyocytes were isolated from the hearts of 6-12 months old NZW rabbits (both sexes) with standard enzymatic techniques using a Langendorff system. NZW rabbits were administered buprenorphene (0.03 mg/kg IM), a cocktail (IM) of acepromazine (0.5 mg/kg), ketamine (60 mg/kg) and xylazene (15 mg/kg), pentobarbital sodium (50 mg/kg IV), and heparin (300 U/kg IV). The filtered cells were maintained in 45 mM KCl, 65 mM K-glutamate, 3 mM $MgSO_4$, 15 mM KH_2PO_4, 16 mM taurine, 10 mM HEPES, 0.5 mM EGTA, and 10 mM glucose (pH 7.3) for one hour. Cells were centrifuged, resuspended in medium 199 supplemented with 5% FBS and antibiotics and plated on laminin-coated cover glasses. After 2-3h, the medium was replaced and adenovirus [50 multiplicity of infection (MOI)] added to the cells. Cells were maintained at 37°C with 5% CO_2 and approximately 48 h later, cells were used for calcium cycling experiments.

3-week-old ventricular cardiomyocytes were isolated from the hearts of 3-week-old NZW rabbits (both sexes) with standard enzymatic techniques using a Langendorff system. NZW rabbits were administered pentobarbital sodium (65 mg/kg IP) and heparin (1,000 U/kg IP). The filtered cells were maintained in 45 mM KCl, 65 mM K-glutamate, 3 mM $MgSO_4$, 15 mM KH_2PO_4, 16 mM taurine, 10 mM HEPES, 0.5 mM EGTA, and 10 mM glucose (pH 7.3) for half an hour. In five subsequent steps, the Ca^{2+} concentration was increased to 1.8 mM. Cells were centrifuged, resuspended in DMEM supplemented with 7% FBS and antibiotics, plated on laminin-coated cover glasses or tissue culture dishes. After 2-3h, the medium was replaced and adenovirus (50 MOI) added to the cells. Cells were maintained at 37°C with 5% CO_2 and approximately 48 h later, cells were used for patch clamping and biochemistry.

To obtain **neonatal rabbit cardiomyocytes**, neonatal NZW rabbit kits (both sexes, 3–5 days old) were administered pentobarbital sodium (65 mg/kg IP) and heparin (1,000 U/kg IP). After anesthesia, the heart was excised, mounted on a Langendorff system, and perfused with a Ca^{2+}-free solution containing 140 mM NaCl, 4.4 mM KCl, 1.5 mM $MgCl_2$, 0.33 mM NaH_2PO_4, 16 mM taurine, 5 mM HEPES, 5 mM pyruvic acid, and 7.5 mM glucose for 7 min. Then, 0.3 mg/ml collagenase I (Worthington

Biochemical Corporation) was added to the solution and perfused for 4–5 min at a flow rate of 3 ml/min. Ventricles were separated and minced in KB-EDTA [45 mM KCl, 65 mM K-glutamate, 3 mM MgSO4, 15 mM KH_2PO_4, 16 mM taurine, 10 mM HEPES, 0.5 mM EDTA, 10 mM glucose, and 1% BSA (MilliporeSigma) (pH 7.3)]. The cell suspension was filtered and cells were allowed to settle for 1 h at room temperature, yielding 30 million cells/heart. After removal of the supernatant and subsequent centrifugation, the cell pellet was resuspended in Ca^{2+}-free MEM (Lonza) and gradually acclimated to a final Ca^{2+} concentration of 1.8 mM over the course of 20 min. Cells were plated on laminin-coated tissue culture dishes at 100,000 cells/cm^2. Three hours postplating, media was replaced with culture media (DMEM, 7% FBS, 2mM L-glutamine, 1% pen-strep, Thermo Fisher) containing 100 μM BrdU (MilliporeSigma). Cells were maintained under standard culture conditions and fed with culture media and BrdU every other day. After 4 days, when cells reached confluency, the medium was replaced and adenovirus (10 MOI) added. Cells were maintained at 37°C with 5% CO_2 and approximately 48 h later, cells were used for optical imaging and biochemistry.

Immunoblot analysis and co-immunoprecipitation

Co-immunoprecipitations and immunoblot analyses were carried out as previously described.[1] For co-immunoprecipitations, anti-HA antibody (Thermo Fisher; 26183; mouse; 1:100) or control IgG (Santa Cruz Biotechnology) was added to the whole cell lysate and incubated with agitation at 4°C overnight. After extensive washes, eluted proteins were subjected to SDS-PAGE and transferred to nitrocellulose membranes. Blots were incubated with antibodies diluted in phosphate buffered saline containing 5% nonfat milk and 0.1% Tween-20. The following antibodies were used: anti-HA (Thermo Fisher; 26183; mouse; 1:1,000), anti-GAPDH (MilliporeSigma; G8795; mouse; 1:10,000), anti-tubulin (MilliporeSigma; T6199; mouse; 1:10,000), anti-Cavα1c (Alomone; acc-003; rabbit; 1:1,000), anti-Cavβ3 (Alomone; acc-008; rabbit; 1:1,000), anti-Cavβ2 (abnova; PAB9800; rabbit; 1:1000), anti-Cavα2δ-1 (abcam; ab2864; mouse; 1:1,000), anti-LITAF (BD Biosciences; 611614; mouse; 1:1,000), anti-NEDD4-1 (Cell Signaling Technology; 2740; rabbit; 1:1,000), anti-SERCA2 (Thermo Fisher; MA3-910; mouse; 1:1,000), anti-NCX (Thermo Fisher; MA3-926; mouse; 1:1,000), anti-CSQ2 (MilliporeSigma; C3868; rabbit; 1:1,000), and anti-transferrin receptor (Novus Biologicals; NB100-92243; rabbit; 1:1,000). The binding of the primary antibody to proteins was detected using HRP-conjugated secondary antibody followed by ECL detection (Thermo Fisher). The chemiluminescent blots were imaged with the ChemiDoc MP imager (Bio-Rad). The ImageLab software version 6.0 (Bio-Rad) was used for image acquisition and densitometric analysis of the respective blots.

In situ proximity ligation assay

For PLA, 3wRbCM were plated on 12-mm laminin-coated circular glass coverslips and cultured for 3-5 hours in 24-well plates. Cells were fixed with 4% paraformaldehyde at

room temperature for 15 min followed by permeabilization at room temperature with 0.1% triton X-100 for 10 min prior to the assay. PLA was performed according to the manufacturer's instructions (Sigma: Duolink® In Situ Red Starter Kit Mouse/Rabbit). After five washes with PBS, cells were blocked for 30 min at 37°C. Antibodies used for PLA were as follows: rabbit anti-Cavα1c (Alomone; acc-003; 1:100); mouse anti-LITAF (abnova; H00009516-B01P; 1:100); mouse anti-Cavα1c (Invitrogen; MA5-27717; 1:100); rabbit anti-LITAF (abcam; ab224066; 1:100); rabbit anti-Cavα2δ-1 (Sigma; C5105; 1;200); mouse anti-Cavα2δ-1 (abcam; ab2864; 1;200). The latter two antibodies were used as positive control to detect endogenous Cavα2δ-1. Images were captured using Elements software (Nikon), TRITC emission filters, and a monochromatic camera.

Aquaculture

Experiments were performed on zebrafish (*D. rerio*) from wild-type (WT) AB/Tuebingen breeding colonies in accordance with animal protocols approved by the Harvard Medical School Institutional Animal Care and Use Committee (reference number: 2016N000276). Care and breeding of zebrafish were performed as described previously at 28.5°C with standard media (E3).[6]

Morpholino knockdown

Antisense morpholino oligomers (Gene Tools LLC) were designed to target the start codon of the LITAF ortholog. The specific sequence was 5' TCGGCATCGGCATCGCCATCGTTGT 3'. The morpholino was resuspended in 1x Danieu's solution to a stock concentration of 1 mM and then diluted into working solutions between 300 µM and 500 µM. About 1 nl of morpholino was injected into fertilized eggs from TuAB fish at the single cell stage. The effectiveness of splice targeting morpholinos was assessed by qRT-PCR (data not shown). As an additional measure of morpholino specificity, we tested all of the morpholinos used in the setting of p53 knockdown to verify that the phenotypes seen in wild-type embryos were not secondary to non-specific activation of p53.[7]

Intracellular Ca^{2+} transient measurements in zebrafish embryo hearts

These measurements have been described in detail elsewhere.[8] Briefly, individual hearts from 48 hours post fertilization (hpf) old wild-type (WT) and LITAF morphant zebrafish embryos were isolated by microdissection in Tyrode's solution (TS), which contained 136 mM NaCl, 5.4 mM KCl, 0.3 mM NaH_2PO_4, 1.8 mM $CaCl_2$,1 mM $MgCl_2$, 5 mM glucose, 10 mM HEPES, and 2 % BSA. The solution pH was adjusted to 7.4 with NaOH. Cardiac motion was arrested with 10 µM blebbistatin. Hearts were stained for 15 minutes with the Ca^{2+}-sensitive dye Fura-2 AM (Thermo Fisher) and subsequently

washed in dye-free TS. After 45 minutes of incubation at room temperature to allow complete intracellular hydrolysis of the esterified dye, hearts were placed into a recording chamber with integrated field stimulation electrodes (Warner Instruments RC-27). To illuminate the stained hearts, a monochromator was used to rapidly switch the excitation wavelength between 340 nm and 380 nm with a bandwidth of 20 nm at a frequency of 500 Hz. The excitation light was reflected by a 400 nm cutoff dichroic mirror, and fluorescence emission (510/80 nm emission filter) was collected by an 80 x 80 pixel high-speed CCD camera (CardioCCF-SMQ, RedShirtImagin, LLC).

Electrophysiological recordings of 3-week-old rabbit cardiomyocytes

3-week-old rabbit cardiomyocytes were transduced with adenovirus 44 to 50 hours before whole-cell $I_{Ca,L}$ recording. The current was recorded at 34-36°C with Axopatch-200B amplifier and Digidata 1440A (Axon Instruments). The signal was acquired at 20 kHz and filtered at 5 kHz and with pClamp 10 (Axon Instruments). Tyrode solution was used as a standard bath solution and contained 140 mM NaCl, 5.4 mM KCl, 0.33 mM NaH_2PO_4, 1 mM $CaCl_2$, 1 mM $MgCl_2$, 5 mM HEPES, and 7.5 mM D-glucose (pH 7.4). The pipette solution contained 105 mM CsCl, 10 mM tetraethylammonium chloride, 4 mM $MgCl_2$, 10 mM EGTA, 10 mM HEPES, 4 mM Mg-ATP, and 10 phosphcreatine-Na_2 (pH 7.2). The pipette resistance was 2-4 MΩ. The $I_{Ca,L}$ current was activated by 300 ms depolarizing pulses (from -50 to +60 mV, with 10 mV increments) from the -50 mV holding potential. The leak current was subtracted with standard P/8 protocol. After the cell membrane was broken by application of additional suction, cell capacitance and series resistance were electrically compensated. Current amplitudes were normalized to the cell capacitance and expressed as pA/pF. To study inactivation of $I_{Ca,L}$, a 300-ms conditioning pulse (to voltages from −70 to +50 mV, 10 mV steps) was applied, followed by a 300 ms step to −50 mV before the 300 ms test pulse to +10 mV. Again, the holding potential was −50 mV. Currents were measured relative to the peak current at the test potential after the conditioning potential of −70 mV (I max). Linear leakage and capacitance transients were eliminated by a standard subtraction protocol. Currents were filtered by a low-pass filter with cut-off frequency of 2 kHz and sampled at 10 kHz.

Confocal microscopy measurements of Ca^{2+} transients

Intracellular Ca^{2+} cycling and intra-SR Ca^{2+} cycling in transduced adult rabbit cardiomyocytes were monitored by a Leica SP2 confocal laser scanning system equipped with a x60 1.4 NA oil-immersion objective in linescan and x–y mode using Ca^{2+}-sensitive indicators Fluo-3, Fluo-5N, and Fluo-4 (Thermo Fisher), respectively. For intracellular Ca^{2+} cycling measurements, cells were loaded with Fluo-3 for 12 min, and after 20 min de-esterification, the dye was excited with the 488 nm line of an argon laser. Emission was collected at 500–600 nm. Cardiomyocytes were studied in Tyrode solution (140 mM NaCl, 5.4 mM KCl, 1.8 mM $CaCl_2$, 0.5 mM $MgCl_2$, 10 mM HEPES, and 5.6 mM glucose, pH = 7.3) at baseline and with 30 nM isoproterenol, a β-adrenergic

receptor agonist. Cells were paced via field stimulation at 1 Hz using extracellular platinum electrodes. To assess the SR Ca^{2+} load and decay kinetics, 20 mM caffeine was applied at the end of the experiments. Sodium-calcium exchanger (NCX) activity was estimated by measuring the rate of decay of caffeine-induced Ca^{2+} transients (k_{caff}), and SR (ER) Ca^{2+}-ATPase (SERCA2) activity was estimated via a derived rate of decay (k_{SR}) by subtracting the rate of decay of caffeine-induced Ca^{2+} transients (k_{caff}) from the rate of decay of pacing-induced Ca^{2+} transients as described previously.[9, 10]

Reverse transcription and real-time PCR

Reverse transcription was performed using the iScript™ Reverse Transcription Supermix for RT-qPCR (Bio-Rad), following the manufacturer's protocol and 1 µg of each RNA sample prepared from transduced neonatal rabbit cardiomyocytes. The cDNA was stored at -20°C and quantitative real-time PCR was performed with a 7500 Fast Real-Time PCR System (Applied Biosystems). Each assay sample was run in triplicate. PrimePCR SYBR Green Assays from Bio-Rad (rabbit CACNA1A, Assay ID: qOcuCID0002288 and rabbit SRP14, Assay ID: qOcuCID0013315) were used according to the manufacturer's recommendations. Cycling parameters were as follows: initial polymerase activation step (10 min at 95°C), followed by 2-step cycling for 40 cycles (15 s at 95°C and 1 min at 60°C). 20 µl reactions were composed of iTaq™ Universal SYBR® Green Supermix and 100 ng cDNA (CACNA1A). Respective Ct values were normalized to SRP14 (100 ng). The relative expression of CACNA1A was calculated using the ΔΔCt method.

Rabbit ventricular myocyte model

To study the effect of LITAF in LMC myocytes, we used a physiologically detailed rabbit ventricular myocyte model of Zhong *et al*.[11] This model is based on earlier models developed by Restrepo *et al*.[12] and further improved by Terentyev *et al*.[13] Combining together a large number of ~ 16,000 diffusively coupled Ca^{2+} release units (CRU), this multi-scale model successfully links the whole cell level Ca^{2+} dynamics to the local subcellular Ca^{2+} dynamics in each CRU, which incorporates 4 long-type Ca^{2+} channels (LTCC) and 100 ryanodine receptors (RyR), both implemented by Markov models. By including the Ca^{2+} dependent channels LTCC and Na^{+}-Ca^{2+} exchanger and other sarcolemmal currents, this detailed model describes the bi-directional coupling of Ca^{2+}-V_m dynamics, which is essential in cardiac electrophysiological behavior.

The $I_{Ca,L}$ channels described by the 16-state Markov model can be reduced to the standard Hodgkin-Huxley model with constant opening rate, voltage dependent Ca^{2+} activation, voltage dependent inactivation and local dyadic space Ca^{2+} dependent inactivation. The results of this model show a good agreement with the voltage clamped experiment data in Terentyev *et al*.[13] For the RyR channels, we used a 4-state Markov model which incorporates the refractoriness associated with CSQN unbinding from triadin-1/junctin. The details of LTCC model and RyR model are shown in Zhong *et al*.[11]

We first carried out the voltage clamp simulations, with the $I_{Ca,L}$ conductance varied to match the peak $I_{Ca,L}$ versus voltage curves measured for rabbit myocytes with GFP and LITAF (Figure 2B). Then we carried out the current clamp simulations by pacing the myocytes at 2.5 Hz (400 ms), where the intracellular sodium concentration reached the steady state before the data were collected.

Based on Zhong *et al*,[11] we applied the modifications described by the following paragraphs. All the modified parameters are listed in Table S1.

(1) In the cell transduced with adenovirus encoding with LITAF, there is a decrease of Cavα1c protein levels compared to the cell with GFP. This result suggests that the total number of LCCs in the cell is smaller for LITAF, while the single channel current is kept the same. Therefore, we reduced the number of LCCs in a dyad by half to mimic the different level of Cavα1c abundance.

(2) Following Shannon *et al*,[14] we adopted that intracellular $[Na^{+}]$ dependence of the Na^{+}/K^{+} pump current (I_{NaK}) is a Hill function with the power equal to 4, which is supported by previous experiment.[15] The model is described as Eq. 1.

$$\sigma = \frac{\exp\left(\frac{[Na]_o}{67.3}\right) - 1}{7}$$
$$f_{NaK} = \frac{1}{1 + 0.1245\exp\left(-0.1\frac{VF}{RT}\right) + 0.0365\sigma\exp\left(-\frac{VF}{RT}\right)} \quad (1)$$

$$I_{NaK} = \frac{\bar{I}_{NaK} Q_{NaK} f_{NaK}}{1 + \left(\frac{Q_{KmNai} K_{mNai}}{[Na]_i}\right)^{H_{NaK}}} \frac{[K]_o}{[K]_o + K_{mKo}}$$

(3) Cytosolic volume

The data in D.M. Bers[16] and Satoh *et al*.[17] showed that ~ 30% of cytosolic space is occupied by mitochondria, which implies that the effective cytosolic space for Ca^{2+} diffusion is ~ 1 μm^3, considering that the average distance between z-lines is 1.8 μm and the average distance between dyadic spaces in the transverse direction is 0.9 μm. Hence, we increased the effective cytosolic space volume per CRU from 0.5 μm^3 to 1 μm^3 to make the model more realistic.

(4) RyR gating

With increase of cytosolic space volume, more amount of buffer is present in the cell, which results in a smaller amplitude of Ca^{2+} transient during pacing and less Ca^{2+} dependent inactivation of LTCC. In order to counterbalance this effect, we modified the RyR open probability and Ca^{2+} sensitivity so that Ca^{2+} transient was reasonable.

(5) Allosteric Ca^{2+} activation of NCX

Following Mahajan *et al*.[18], we used the simpler formulation of NCX current, where the allosteric Ca^{2+} activation is independent of time.

(6) Voltage dependent inactivation time scale τ_f of $I_{Ca,L}$

We modified the voltage dependent inactivation time scale with the parameter f_{τ_f} shifted from 1 to 1.2.

$$\tau_f = \frac{f_{\tau_f}}{0.02 - 0.007\, e^{-(0.0337(V_m+10.5))^2}}$$

Table S1. Modified parameters in the model

Parameter	Definition	Value
n_{LCC} (GFP)	Number of LCCs in a dyad	4
n_{LCC} (LITAF)	Number of LCCs in a dyad	2
P_{Ca}	LCC permeability	$15.2\ \mu mol/(cm\ C)$
$\bar{I}_{NaK}$	I_{NaK} conductance	$1.91\ pA/pF$
Q_{NaK}	Constant in I_{NaK} function	1
Q_{KmNai}	Constant in I_{NaK} function	1
K_{mNai}	$[Na^+]_i$ sensitivity in I_{NaK} function	$11\ mM$
H_{NaK}	Hill coefficient in I_{NaK} function	4
g_{Ks}	I_{Ks} conductance	$0.4\ mS/\mu F$
g_{NCX}	Strength of I_{NCX}	$21\ \mu M/ms$
g_{leak}	SR leak strength	$2.07 \times 10^{-5} ms^{-1}$
τ_u	Time scale of CSQN unbinding	$1100\ ms$
τ_b	Time scale of CSQN binding	$1\ ms$
τ_{il}	Diffusion time between 2 compartments of cytosol in longitudinal direction	$0.49\ ms$
τ_{it}	Diffusion time between 2 compartments of cytosol in transverse direction	$0.231\ ms$
B_{SAR}	Sarcolemma Ca^{2+} binding site concentration	$42\ \mu mol/l\ cyt$
B_{MH}	Membrane high Ca^{2+} binding site concentration	$15\ \mu mol/l\ cyt$
V_i	Cytosolic space volume	$1\ \mu m^3$
$\bar{k}_{p,U}$	Constant of RyR unbound state open rate	$80\ ms^{-1}$
$\bar{k}_{p,B}$	Constant of RyR bound state open rate	$35.5\ ms^{-1}$
c^*	Ca^{2+} sensitivity parameter of RyR	$19\ \mu M$

Statistical analysis

Statistical analysis of biochemical, electrophysiological and Ca^{2+} imaging data was performed using Origin 8.0 (OriginLab), GraphPad Prism or Microsoft Excel. Data are presented as mean ± standard error of the mean (S.E.M) or standard deviation (S.D.). Statistical comparisons between groups were performed with Fisher exact test, Student's *t*-test (paired and unpaired) and one-way ANOVA with post hoc test (Bonferroni) where appropriate. For all analyses, differences were considered statistically significant at $p<0.05$.

Supplemental References

1. Roder K, Werdich AA, Li W, Liu M, Kim TY, Organ-Darling LE, Moshal KS, Hwang JM, Lu Y, Choi BR, MacRae CA, Koren G. Ring finger protein rnf207, a novel regulator of cardiac excitation. *J Biol Chem*. 2014;289:33730-33740

2. Lim KL, Chew KC, Tan JM, Wang C, Chung KK, Zhang Y, Tanaka Y, Smith W, Engelender S, Ross CA, Dawson VL, Dawson TM. Parkin mediates nonclassical, proteasomal-independent ubiquitination of synphilin-1: Implications for lewy body formation. *J Neurosci*. 2005;25:2002-2009

3. Helton TD, Xu W, Lipscombe D. Neuronal l-type calcium channels open quickly and are inhibited slowly. *J Neurosci*. 2005;25:10247-10251

4. Lin Y, McDonough SI, Lipscombe D. Alternative splicing in the voltage-sensing region of n-type cav2.2 channels modulates channel kinetics. *J Neurophysiol*. 2004;92:2820-2830

5. Gao S, Alarcón C, Sapkota G, Rahman S, Chen PY, Goerner N, Macias MJ, Erdjument-Bromage H, Tempst P, Massagué J. Ubiquitin ligase nedd4l targets activated smad2/3 to limit tgf-beta signaling. *Mol Cell*. 2009;36:457-468

6. Panáková D, Werdich AA, Macrae CA. Wnt11 patterns a myocardial electrical gradient through regulation of the l-type ca(2+) channel. *Nature*. 2010;466:874-878

7. Robu ME, Larson JD, Nasevicius A, Beiraghi S, Brenner C, Farber SA, Ekker SC. P53 activation by knockdown technologies. *PLoS Genet*. 2007;3:e78

8. Wythe JD, Jurynec MJ, Urness LD, Jones CA, Sabeh MK, Werdich AA, Sato M, Yost HJ, Grunwald DJ, Macrae CA, Li DY. Hadp1, a newly identified pleckstrin homology domain protein, is required for cardiac contractility in zebrafish. *Dis Model Mech*. 2011;4:607-621

9. Cooper LL, Li W, Lu Y, Centracchio J, Terentyeva R, Koren G, Terentyev D. Redox modification of ryanodine receptors by mitochondria-derived reactive oxygen species contributes to aberrant ca2+ handling in ageing rabbit hearts. *J Physiol*. 2013;591:5895-5911

10. Belevych A, Kubalova Z, Terentyev D, Hamlin RL, Carnes CA, Györke S. Enhanced ryanodine receptor-mediated calcium leak determines reduced sarcoplasmic reticulum calcium content in chronic canine heart failure. *Biophys J*. 2007;93:4083-4092

11. Zhong M, Rees CM, Terentyev D, Choi BR, Koren G, Karma A. Ncx-mediated subcellular ca. *Biophys J*. 2018;115:1019-1032

12. Restrepo JG, Weiss JN, Karma A. Calsequestrin-mediated mechanism for cellular calcium transient alternans. *Biophys J*. 2008;95:3767-3789

13. Terentyev D, Rees CM, Li W, Cooper LL, Jindal HK, Peng X, Lu Y, Terentyeva R, Odening KE, Daley J, Bist K, Choi BR, Karma A, Koren G. Hyperphosphorylation of ryrs underlies triggered activity in transgenic rabbit model of lqt2 syndrome. *Circ Res*. 2014;115:919-928

14. Shannon TR, Wang F, Puglisi J, Weber C, Bers DM. A mathematical treatment of integrated ca dynamics within the ventricular myocyte. *Biophys J*. 2004;87:3351-3371

15. Despa S, Islam MA, Pogwizd SM, Bers DM. Intracellular [na+] and na+ pump rate in rat and rabbit ventricular myocytes. *J Physiol*. 2002;539:133-143

16. Bers DM. Cardiac excitation-contraction coupling. *Nature*. 2002;415:198-205

17. Satoh H, Delbridge LM, Blatter LA, Bers DM. Surface:Volume relationship in cardiac myocytes studied with confocal microscopy and membrane capacitance measurements: Species-dependence and developmental effects. *Biophys J*. 1996;70:1494-1504

18. Mahajan A, Shiferaw Y, Sato D, Baher A, Olcese R, Xie LH, Yang MJ, Chen PS, Restrepo JG, Karma A, Garfinkel A, Qu Z, Weiss JN. A rabbit ventricular action potential model replicating cardiac dynamics at rapid heart rates. *Biophys J*. 2008;94:392-410

19. Consortium G. The genotype-tissue expression (gtex) project. *Nat Genet*. 2013;45:580-585

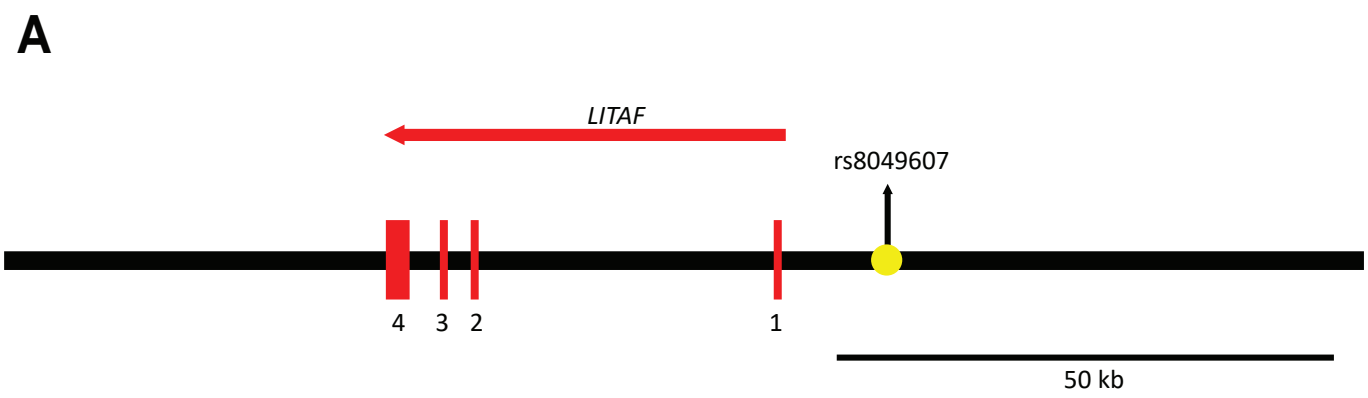

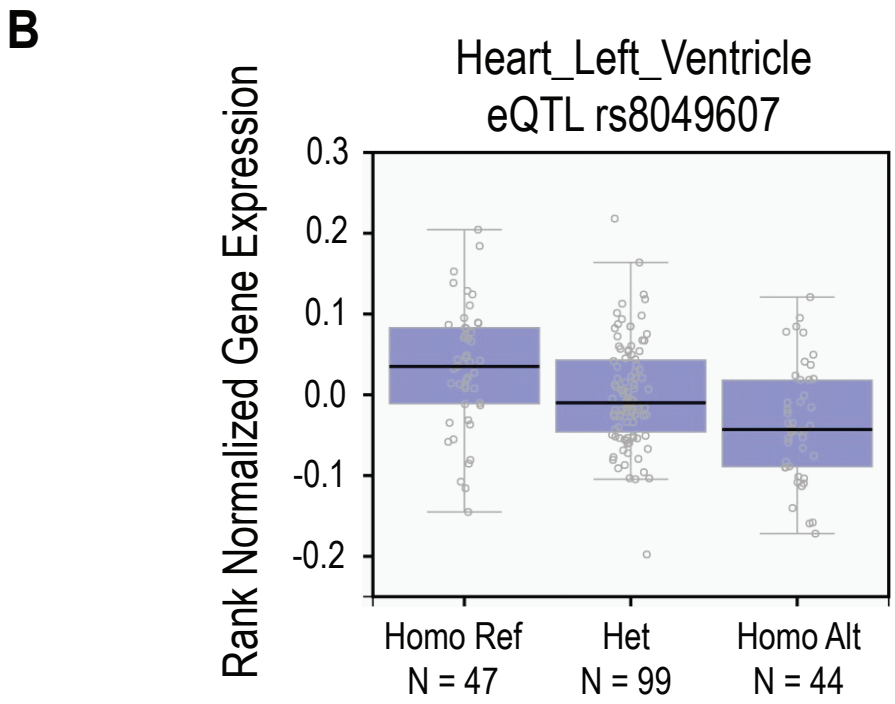

Figure I. rs8049607 is associated with lower levels of LITAF mRNA in the left ventricle. *A*, Schematic of the *LITAF* gene locus and location of the SNP associated with QT interval duration: rs8049607 is approximately 41 kb upstream of the LITAF start codon[19] and located within an intergenic enhancer region.[20] The four exons are represented by numbered red rectangles. The yellow circle indicates rs8049607-surrounding chromatin with a DNase I hypersensitivity cluster, histone H3K27 acetylation and various transcription factor binding sites, which are based on data from the ENCODE project using various cell lines.[21-23] *B*, eQTL data from the GTEx project[24] show that left ventricular heart samples from individuals carrying a heterozygous or homozygous SNP have lower LITAF transcript expression (p=8.2e-8).

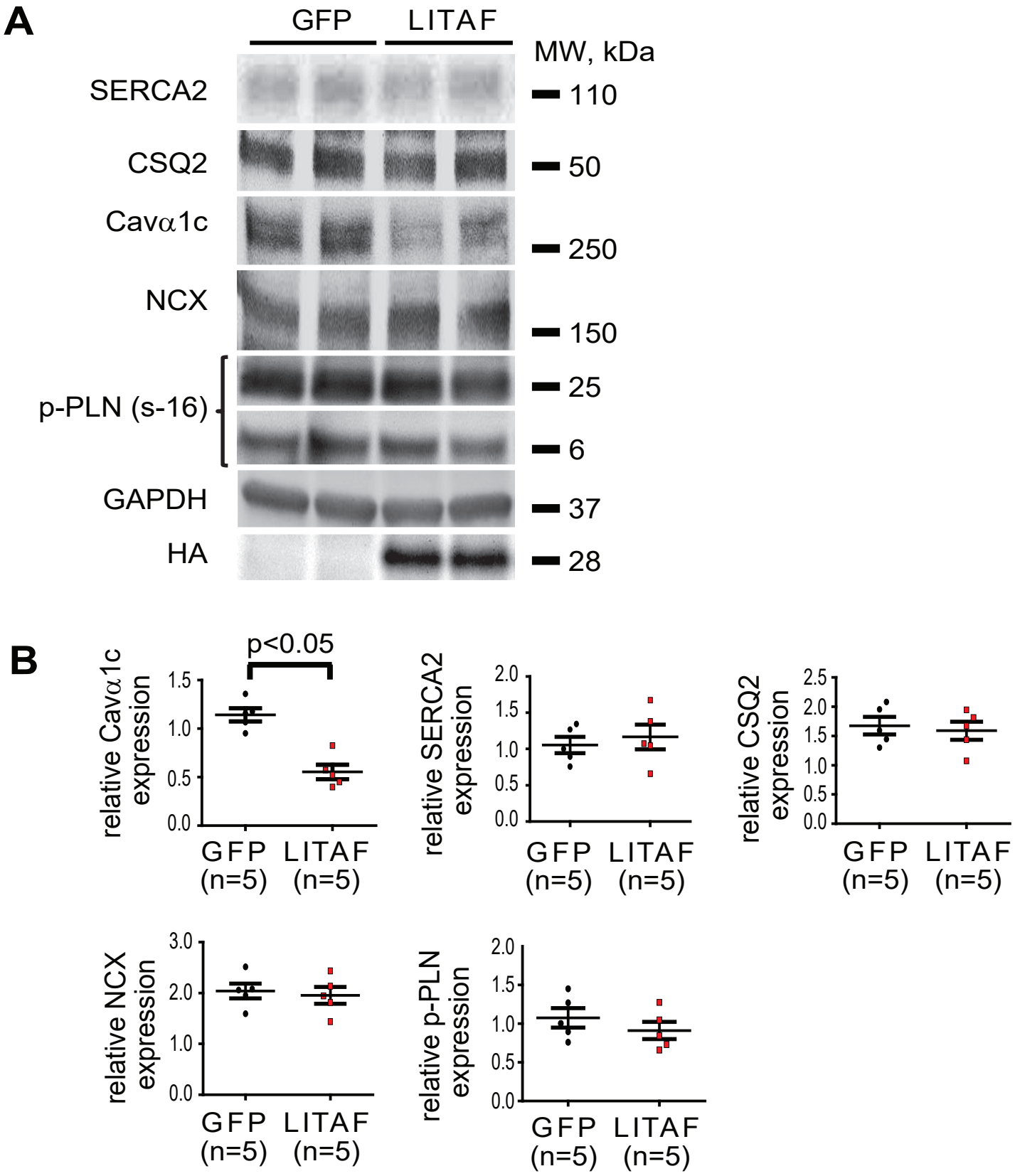

Figure II. Protein levels of SERCA2 or NCX are not affected by LITAF. NRbCM were transduced with adenovirus expressing GFP or LITAF. **A**, Representative protein levels of SERCA2, CSQ2, Cavα1c, NCX, serine 16-phosphorylated phospholamban [p-PLN (s-16)], HA-tagged LITAF, and GAPDH in GFP- and LITAF-overexpressing cells. **B**, Respective changes in total protein levels, normalized to GAPDH levels (n=5, performed in triplicate; mean±SEM). Student's t-test, $p<0.05$.

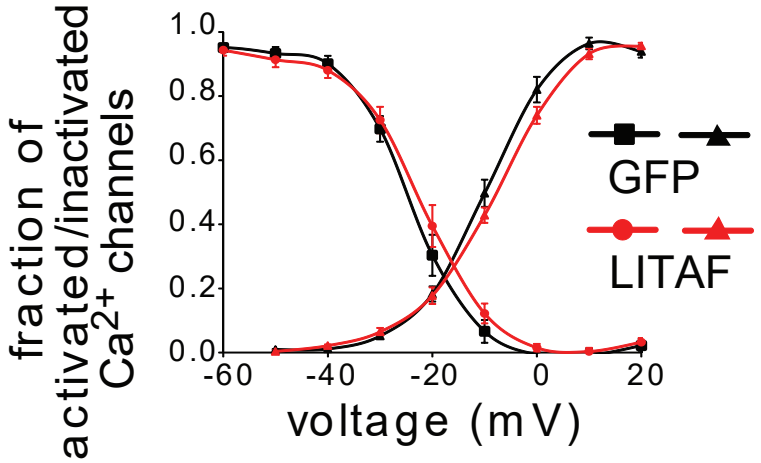

Figure III. LITAF does not affect voltage-dependent activation and inactivation of $I_{Ca,L}$. 3-week-old rabbit cardiomyocytes were transduced with adenovirus encoding GFP or HA-LITAF for 48 h. Voltage-dependent activation and inactivation of $I_{Ca,L}$ was calculated from the respective current traces (n=5; GFP: 17 cells, LITAF: 15 cells; mean±SEM).

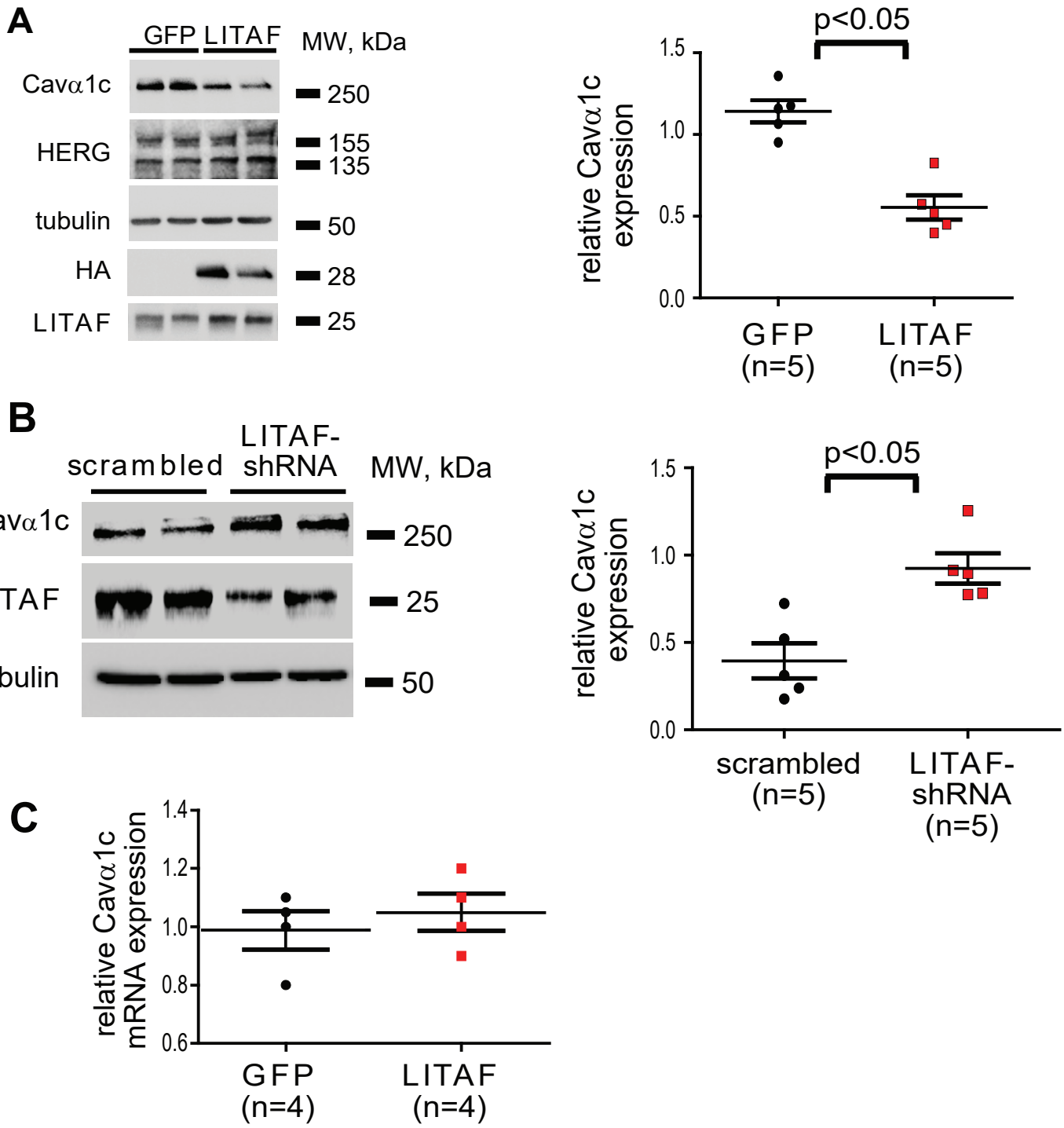

Figure IV. Cavα1c protein but not transcript levels are affected by LITAF overexpression in neonatal rabbit cardiomyocytes. A, Representative protein levels of Cavα1c, HA-tagged LITAF, and tubulin in GFP- and LITAF-overexpressing cells (left panel). Respective change in total Cavα1c abundance, normalized to tubulin levels (n=5, performed in triplicate; mean±SEM) (right panel). **B**, Representative protein levels of Cavα1c, LITAF, and tubulin in NRbCM transduced with adenovirus encoding scrambled RNA or LITAF shRNA (left panel). Respective change in total Cavα1c abundance, normalized to tubulin levels (n=5 performed in triplicate; mean±SEM) (right panel). **C**, Cavα1c mRNA levels from adenovirally transduced cells expressing GFP as control or LITAF were quantified by qPCR. Values (n = 4 animals, performed in triplicate) refer to the relative -fold change in Cavα1c mRNA levels normalized to SRP14 mRNA levels. Error bars depict standard deviation.

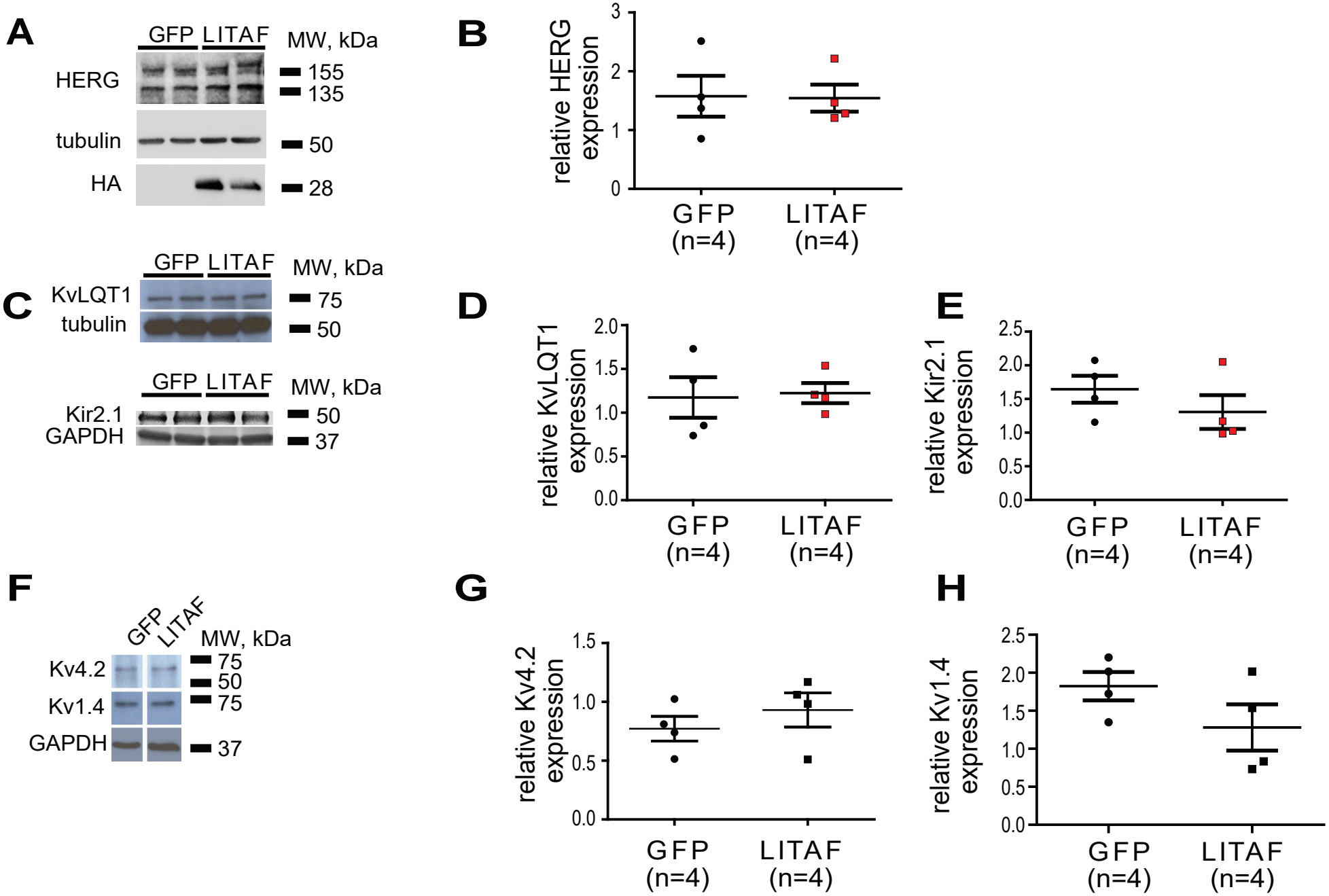

Figure V. LITAF has no effect on cardiac potassium channel levels. A, Protein levels of HERG, HA-tagged LITAF, and tubulin. **B**, Respective change in HERG abundance, normalized to tubulin (n=4 animals, performed in duplicate; mean±SEM). Student's t-test, $p>0.05$. **C**, Protein levels of KvLQT1, Kir2.1, and tubulin. **D-E**, Respective changes in KvLQT1 and Kir2.1 abundance, normalized to tubulin or GAPDH (n=4 animals, performed in duplicate; mean±SEM). Student's t-test, $p>0.05$. **F**, Protein levels of Kv4.2, Kv1.4, and tubulin. **G-H**, Respective changes in Kv4.2 and Kv1.4 abundance, normalized to GAPDH (n=4 animals, performed in duplicate; mean±SEM). Student's t-test, $p>0.05$.

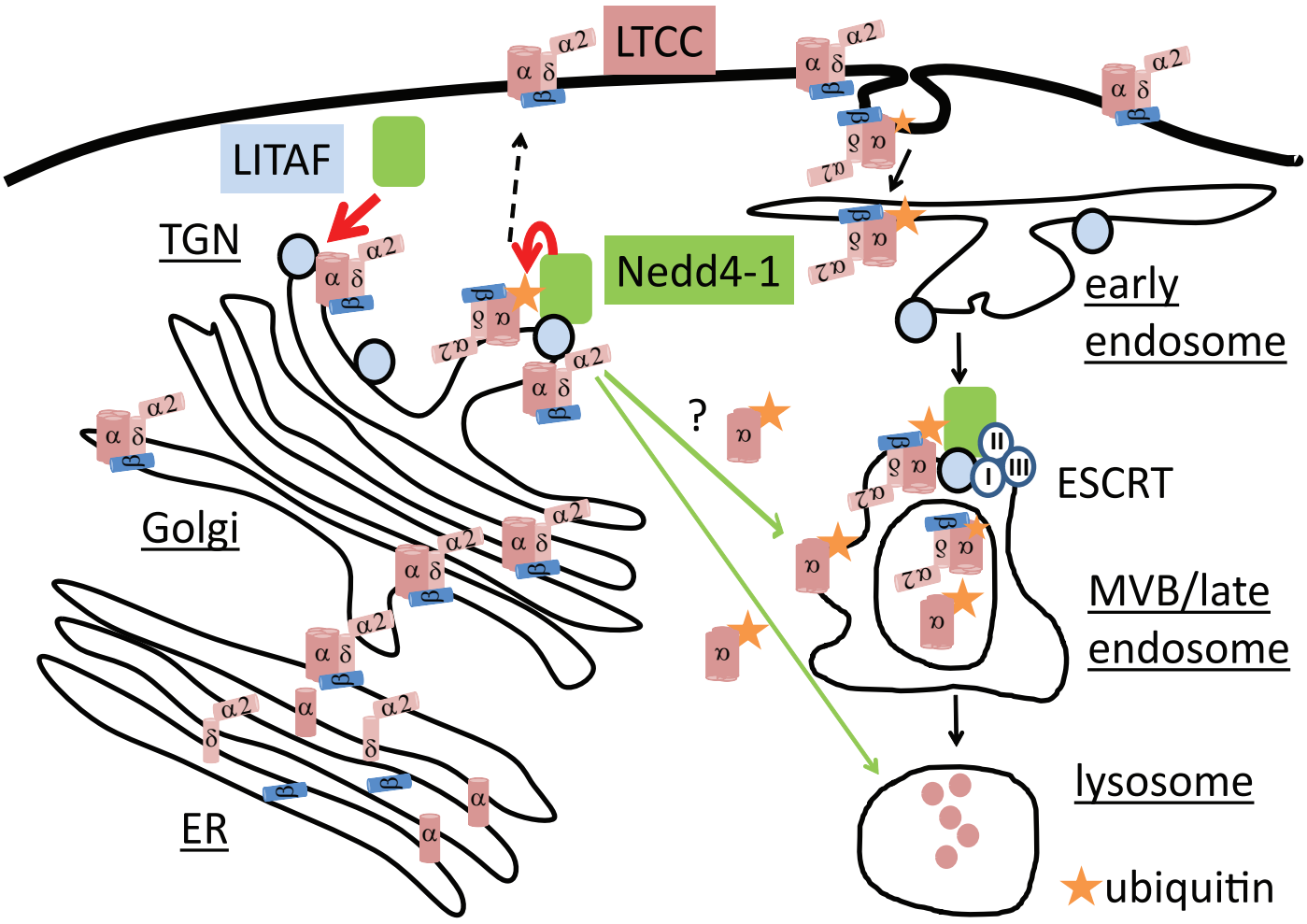

Figure VI. Model of LITAF-mediated degradation of L-type Ca^{2+} channels in the heart. LITAF directs and promotes NEDD4-1-mediated ubiquitination of Cavα1c on the *trans*-Golgi network. Ubiquitination, in turn, serves as signal for lysosomal degradation of Cavα1c. ER, endoplasmic reticulum; MVB, multivesicular body; TGN trans-Golgi network.